

Technical Note

Not peer-reviewed version

Hybrid Control for a 4-Cell PV String: Spintronic Bypass Management with Classical MPPT

[Pietro Perlo](#)*

Posted Date: 16 April 2026

doi: 10.20944/preprints202604.1179.v1

Keywords: photovoltaic string; partial shading; fast-moving shadows; hybrid control; spintronic crossbar; magnetic tunnel junction; MTJ; bypass MOSFET; hot-spot prevention; MPPT; perturb and observe; incremental conductance; boost converter; analog computation; PWM control



Preprints.org is a free multidisciplinary platform providing preprint service that is dedicated to making early versions of research outputs permanently available and citable. Preprints posted at Preprints.org appear in Web of Science, Crossref, Google Scholar, Scilit, Europe PMC.

Copyright: This open access article is published under a [Creative Commons CC BY 4.0 license](#), which permit the free download, distribution, and reuse, provided that the author and preprint are cited in any reuse.

Disclaimer/Publisher's Note: The statements, opinions, and data contained in all publications are solely those of the individual author(s) and contributor(s) and not of MDPI and/or the editor(s). MDPI and/or the editor(s) disclaim responsibility for any injury to people or property resulting from any ideas, methods, instructions, or products referred to in the content.

Technical Note

Hybrid Control for a 4-Cell PV String: Spintronic Bypass Management with Classical MPPT †

Pietro Perlo

Interactive Fully Electrical VehicleS (IFEVS), La Loggia, Italy; pietro.perlo@ifevs.com

† This technical note presents a teaching-scale hybrid control architecture for PV strings under partial shading. The note focuses on system-level principles and educational use, while the per-cell bypass arrangement is retained for clarity of exposition.

Abstract

This report presents a hybrid control architecture for a series-connected string of four photovoltaic cells as a pedagogical exercise. A spintronic 4×4 crossbar is used exclusively to monitor per-cell voltages and activate the corresponding bypass MOSFETs in nanoseconds, while a conventional digital microcontroller runs a classical MPPT algorithm for string-level optimization. The note uses this hybrid “crossbar bypass + digital MPPT” architecture as an educational case study for PV shadow management.

Keywords: photovoltaic string; partial shading; fast-moving shadows; hybrid control; spintronic crossbar; magnetic tunnel junction; MTJ; bypass MOSFET; hot-spot prevention; MPPT; perturb and observe; incremental conductance; boost converter; analog computation; PWM control

1. Introduction

In a series-connected PV string, fast bypass of shaded cells is essential to prevent hot-spots and to allow the remaining cells to continue delivering power. Conventional digital microcontrollers (MCUs) sample voltages sequentially, apply filtering, and execute iterative decision loops, resulting in latencies of hundreds of microseconds to milliseconds. For fast-moving shadows, this delay can cause reverse bias and energy loss.

A spintronic crossbar array can perform parallel analog computation, reading all cell voltages simultaneously and instantly identifying the weakest cell. This makes it ideal for bypass control. However, MPPT, which requires power calculation, history, and sometimes global scans, is still effectively handled by a digital algorithm.

This report presents a pedagogical exercise that combines the two: the spintronic crossbar handles bypass with nanosecond response, while the MCU runs a standard MPPT algorithm. The exercise is intentionally limited to four cells to keep the explanation simple, but the architecture is generic.

Note on scalability: in traditional digital systems, increasing the number of monitored cells tends to increase sensing, processing, and coordination burden. In a spintronic crossbar, the monitored voltages are evaluated in a single parallel analog step, so the decision path does not grow in the same way as sequential sampling. In practical systems, overall performance will still depend on sensing front-ends, routing, comparator design, and gate-driver implementation. The same hybrid concept can nevertheless be extended to larger strings by using larger crossbars (for example 16×16 or 32×32) and, where appropriate, future multi-level spintronic devices.

2. System Architecture

The system comprises:

- Four series-connected monocrystalline PV cells.

- Four MOSFET bypass switches (Q1–Q4), each across one cell.
- A spintronic 4×4 crossbar that reads the four cell voltages V_{c1} – V_{c4} and performs an analog matrix-vector computation (MVM).
- Four current-to-voltage conversion stages (for example sense resistors or TIAs) and comparators that compare the crossbar outputs to programmable thresholds.
- A digital microcontroller (MCU) that reads string voltage V_{PV} and string current I_{PV} directly from the main power lines, executes a classical MPPT algorithm (P&O or IncCond), sends a duty cycle D (PWM) to the DC-DC converter control input, provides a programming/control line to the crossbar to set the conductance matrix G once at startup or periodically, and can optionally receive a `BYPASS_EVENT` digital flag when any Q_k changes state.
- A DC-DC converter (boost or isolated step-up) that interfaces the PV string to a 36 V battery or DC bus.

Implementation note (converter realism): boosting directly from about 2–3 V (4 cells) to 36 V requires very high duty cycle and high input current, making efficiency and control more difficult. For laboratory demonstrations it is often easier to use clusters, for example 4 clusters in series, where each cluster contains 4 cells in series. This raises the PV input voltage to about 8–9 V at MPP and reduces converter stress. The hybrid bypass/MPPT control principles described here remain the same; only the power-stage design becomes easier.

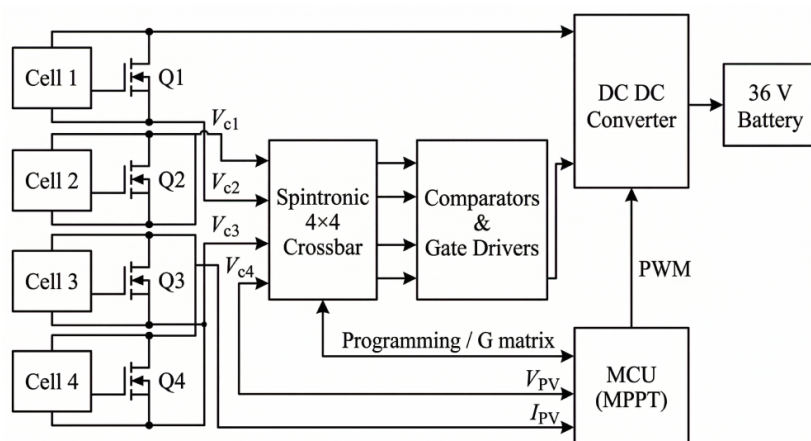


Figure 1. Simplified block diagram of the hybrid control system. The spintronic crossbar reads V_{c1} – V_{c4} and drives comparators that directly trigger bypass MOSFETs. The MCU reads V_{PV} and I_{PV} directly, runs MPPT, and outputs PWM to the DC-DC converter. A single programming link from the MCU sets the crossbar conductance matrix G .

3. Spintronic Crossbar for Bypass Control

3.1. Principle and Mathematical Formulation

The crossbar is programmed with a conductance matrix G so that each output channel produces a signal proportional to how much one cell voltage deviates from the string average. The four input voltages are the per-cell voltages V_{c1} – V_{c4} measured across each cell.

Define the average cell voltage and deviations as $V_{avg} = (V_{c1} + V_{c2} + V_{c3} + V_{c4}) / 4$ and $\Delta V_k = V_{ck} - V_{avg}$.

One convenient choice is $I = G \cdot V$ with $G = g \cdot (I_4 - (1/4) \cdot 11^T)$. For $N = 4$ this becomes:

$$G = g \cdot \begin{bmatrix} 3/4 & -1/4 & -1/4 & -1/4 \\ -1/4 & 3/4 & -1/4 & -1/4 \\ -1/4 & -1/4 & 3/4 & -1/4 \\ -1/4 & -1/4 & -1/4 & 3/4 \end{bmatrix}$$

so that each output current is $I_k = \sum_j G_{kj} \cdot V_{cj} = g \cdot \Delta V_k$ (up to the scale factor g).

Each crossbar column output is a current I_k . In practice it is converted to a voltage using a sense resistor or a transimpedance amplifier (TIA): $V_{k,out} = R_{TIA} \cdot I_k$. A comparator then triggers bypass when $V_{k,out} < -V_{TH}$ (equivalently $I_k < -I_{TH}$). A negative deviation ($\Delta V_k < 0$) means cell k is below the average; bypass is enabled only when the deviation exceeds a chosen margin to avoid triggering on normal mismatch.

3.2. Operation

- **Parallel read:** all cell voltages are applied to the crossbar rows simultaneously.
- **Analog computation:** output currents are generated in nanoseconds.
- **Comparison:** comparators immediately trigger gate drivers.

Turn-ON (protection) rule: when a cell becomes heavily shaded, its voltage collapses. The comparator outputs can directly enable bypass MOSFET Q_k within less than 100 ns when $V_{k,out} < V_{ON}$, with V_{ON} a negative threshold corresponding to $\Delta V_k < -\Delta V_{TH}$, or when the raw cell voltage V_{ck} approaches a safe reverse-bias limit V_{REV} (about 0 V). To avoid chatter under fast shadows and noise, use hysteresis ($V_{ON} < V_{OFF}$) and/or a latch with a minimum ON time $t_{ON,min}$, for example 1–10 ms. Choose ΔV_{TH} large enough to exceed normal cell mismatch, typically on the order of tens of millivolts depending on sensing accuracy.

Turn-OFF (recovery) rule: with a MOSFET bypass ON, V_{ck} is clamped near 0 V, so the analog path cannot directly tell when the cell has recovered. A simple solution is a periodic PROBE: (1) briefly reduce PV current, for example the MCU decreases D for a boost converter, so the string current is small; (2) open Q_k for a short time t_{PROBE} , for example 50–200 μs , and measure V_{ck} ; (3) if $V_{ck} > V_{OFF}$ for the probe window, keep Q_k OFF, otherwise re-enable Q_k . Repeat every T_{PROBE} , for example 10–50 ms.

Latency: the initial bypass decision is dominated by the comparator and gate-driver delays, typically below 100 ns total. The MCU does not need to sample per-cell voltages; it only (i) programs the crossbar conductance matrix G at startup, optionally updates thresholds, and (ii) runs MPPT on the string measurements. In addition, a bypass event can generate a digital flag to the MCU to accelerate MPPT re-lock.

Implementation notes (practical wiring): per-cell voltages V_{c1} – V_{c4} are floating at different common-mode levels, so sensing typically needs differential front-ends or isolation. Gate drive for Q_2 – Q_4 requires level shifting or isolated drivers because the MOSFET sources are not at ground. An “ideal bypass MOSFET” is often implemented with two back-to-back MOSFETs to avoid unintended conduction through the body diode. Crossbar row inputs must be high-impedance so the sensing network does not load the PV cells.

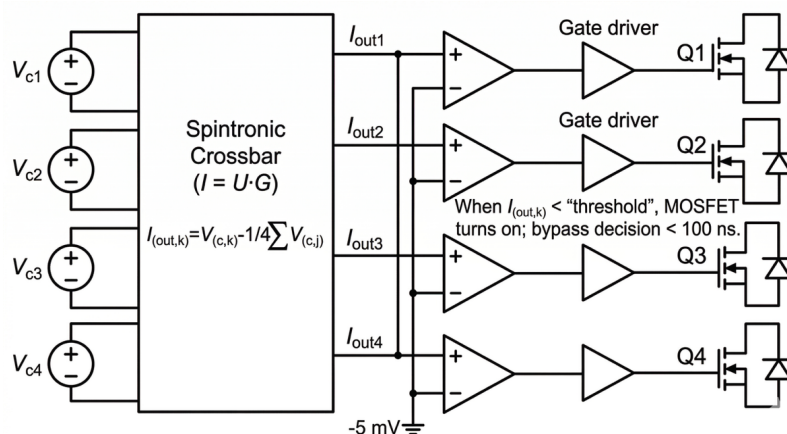


Figure 2. Bypass decision path: V_{c1} – V_{c4} → crossbar → current-to-voltage stage and comparators → gate drivers → MOSFETs. The comparator threshold shown in the schematic is an example after current-to-voltage conversion; in practice it is set to a margin large enough to exceed normal mismatch.

4. Analog-Digital Co-Existence: Why This Split Makes Sense

A key scientific insight of this hybrid architecture is the separation of real-time protection from optimization:

Function	Role
Spintronic crossbar (analog)	Handles the protection task (bypass). This task requires the minimum possible latency to prevent hot-spot damage. The crossbar's parallel analog nature is well suited to this, because it compares all cell voltages in a single step without sampling or iterative loops.
Digital MCU (digital)	Handles the optimization task (MPPT). Tracking the maximum power point involves iterative algorithms, memory of past states, and occasional global scans. Digital logic is flexible, easy to program, and can handle these tasks at a moderate update rate, for example about 10–500 Hz, without needing nanosecond response.

This division of labor leverages the strengths of each technology: the speed of analog for protection and the flexibility of digital for optimization.

5. Classical MPPT in the Digital Domain

The MCU runs a standard MPPT algorithm, such as Perturb & Observe or Incremental Conductance, at a typical update rate of about 10–500 Hz depending on sensor bandwidth and converter dynamics. In many small systems, about 50–200 Hz is common.

It uses the string voltage V_{PV} and current I_{PV} , which reflect the combined effect of active cells and bypass state, and updates the duty cycle D of the DC-DC converter.

Since bypass decisions are made independently, the MPPT algorithm automatically adapts to the new string configuration when a bypass event occurs. For example, when a cell is bypassed the string voltage capability changes and the MPP shifts; the MPPT routine adjusts the duty cycle D to re-lock to the new operating point. Because the MPPT update rate is much slower than the bypass response, there can be a short transient where the system operates away from the MPP until the algorithm catches up. This is why the optional `BYPASS_EVENT` interrupt is helpful.

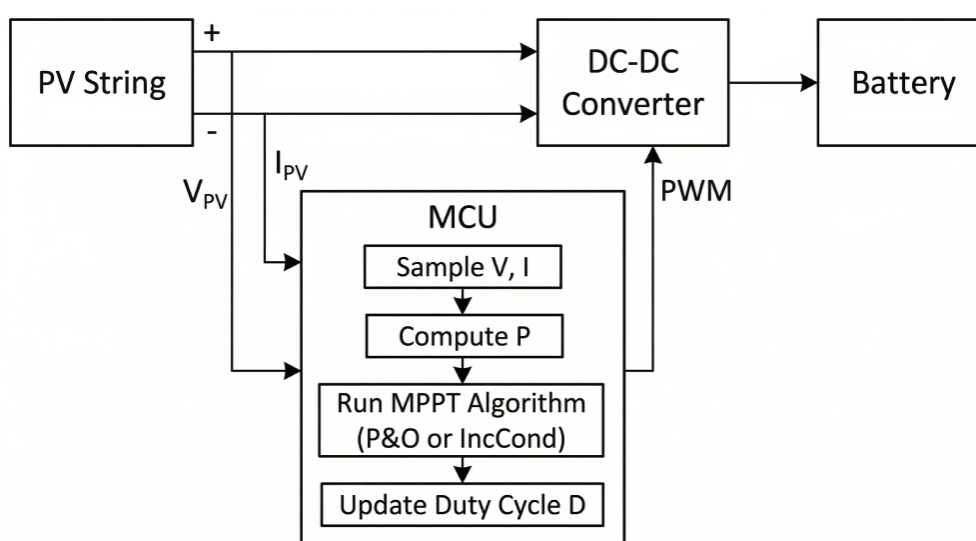


Figure 3. Classical MPPT control loop. The MCU samples V_{PV} and I_{PV} , computes power, runs the MPPT algorithm, and updates the PWM duty cycle.

6. Interaction Between Bypass and MPPT

When a bypass MOSFET turns on or off, the string voltage V_{PV} changes almost instantaneously. The MPPT controller, running at a slower rate, detects the change on the next sample and then adjusts the duty cycle D to track the new MPP. To re-lock faster, the bypass hardware can also raise a digital `BYPASS_EVENT` flag, for example an interrupt to the MCU whenever any Q_k changes state. The MCU can then temporarily increase the MPPT step size or run a short coarse search before returning to normal fine tracking.

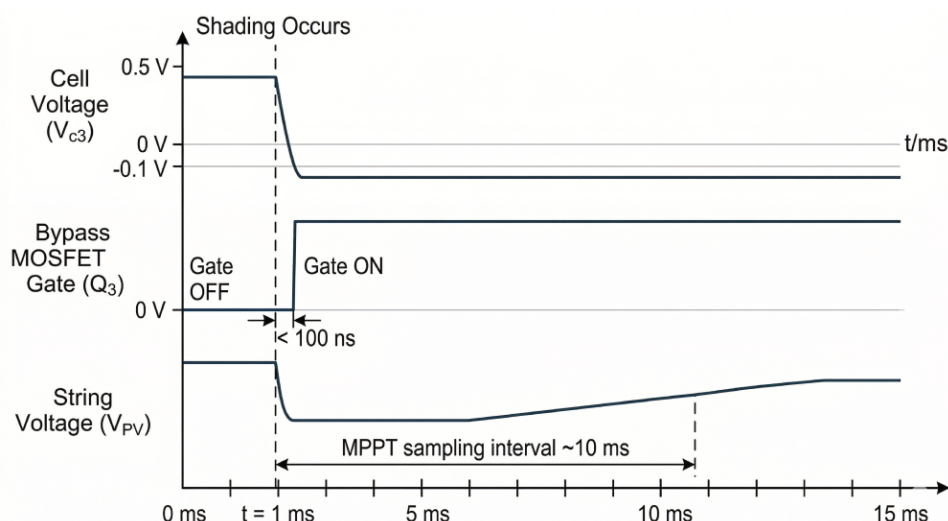


Figure 4. Timing diagram. A shading event triggers bypass in less than 100 ns. The MPPT algorithm detects the voltage drop at the next sampling instant, for example about 10 ms later, and begins tracking the new MPP.

7. Advantages

Advantage	Description
Ultra-fast bypass	Nanosecond response prevents reverse bias and hot-spots.
No cell voltage sampling by MCU	Reduces MCU workload and ADC channels.
Parallel reading	No skew between cell measurements.
Simple MCU code	MPPT algorithm unchanged from classical implementation.
Scalability	The same crossbar can be expanded to more cells without a proportional increase in sequential decision latency, subject to practical sensing and implementation constraints.

8. Limitations

Limitation	Description
MPPT latency	The digital MPPT still introduces a delay, often about 10–100 ms, in adapting to bypass-induced voltage changes, causing brief power loss.
No per-cell MPPT	The crossbar only controls bypass; MPPT is still string-level, so it cannot extract the absolute maximum power under complex shading where different cells have different MPPs.

Additional hardware	Requires a spintronic crossbar and comparators, though the crossbar can be integrated into an ASIC.
Programming complexity	The conductance matrix G must be set appropriately; this may require initial calibration.

9. Comparison with Alternative Architectures

Architecture	Bypass Speed	MPPT Quality	Complexity	Cost
Fully digital MCU	Slow (ms)	String-level	Low	Low
Hybrid (this work)	Fast (ns)	String-level	Medium	Medium
Fully spintronic	Fast (ns)	Per-cell (analog)	High	High

The hybrid approach offers a pragmatic intermediate step: it solves the most critical problem, namely fast bypass, with minimal disruption to existing MPPT designs while keeping the additional hardware manageable.

10. Conclusions

This report has presented a pedagogical exercise in which a spintronic crossbar is used exclusively for fast bypass decisions, while a classical digital MPPT algorithm continues to manage the DC-DC converter. The exercise demonstrates how the parallel analog computation of a spintronic crossbar can achieve nanosecond bypass response, eliminating the risk of hot-spots under fast shading. The digital MPPT retains its flexibility and can be implemented with standard algorithms.

Although we used a 4-cell string with a binary 4×4 crossbar, the principles are generic. The same hybrid architecture can be extended to larger strings by using larger crossbars, for example 16×16 or 32×32, and can incorporate future multi-level spintronic devices for more advanced MPPT.

Looking ahead, this hybrid architecture provides a useful framework for studying how spintronic decision elements may coexist with classical power-electronics control. Future work may explore broader integration of spintronic computing into MPPT and energy-management functions, but those directions should be treated as separate design and validation steps.

11. Economic and Practical Comparison: Hybrid vs Classical Bypass Control

This section compares the practical cost and complexity trade-offs of the proposed hybrid architecture, spintronic crossbar for bypass plus conventional MCU MPPT, against classical solutions. Because prices depend strongly on volume and integration level, the discussion is qualitative and focuses on the main cost drivers.

Reference architectures. For clarity, we compare three common options: classical passive bypass using Schottky diodes plus a conventional MPPT controller; classical active bypass using per-cell sensing plus MCU or FPGA control of MOSFET bypass plus MPPT; and the hybrid approach in which a spintronic crossbar plus fast comparators manage bypass MOSFETs while the MCU keeps a standard MPPT loop.

Cost drivers (hardware). Passive bypass is typically the lowest-cost approach: diodes are cheap and self-actuating, but they dissipate power when conducting. Active MOSFET bypass can reduce conduction losses, but it requires additional circuitry, including per-cell voltage sensing, often floating or differential, gate drivers, often level-shifted or isolated for stacked cells, and a controller fast enough to make stable decisions under rapid transients. The hybrid approach adds the crossbar device and a small analog interface, for example transimpedance and thresholding, but it can reduce the required speed, and sometimes the class, of the MCU because the real-time bypass decision is offloaded to the crossbar.

Cost drivers (engineering time and verification). A major cost in active bypass systems is firmware and verification effort: ensuring correct hysteresis, avoiding chatter, and handling corner cases under fast shadowing. In the hybrid approach, the decision is implemented in a fixed, parallel analog computation once the crossbar conductances are programmed, which can simplify timing analysis. However, the hybrid approach introduces new engineering tasks: calibrating thresholds, validating crossbar programming, and characterizing variability and drift, especially in early prototypes.

Benefit scaling: small vs large PV systems. For small PV systems such as portable, vehicle-mounted, IoT, or educational demonstrators, energy is scarce and shading is often frequent. Here, the hybrid approach can be economically attractive because even modest absolute energy gains translate into meaningful runtime extension, and the additional hardware is limited in count. For large PV installations, the dominant solutions are typically module-level bypass diodes plus string or inverter-level MPPT, and sometimes module-level power electronics. Per-cell bypass rarely scales directly due to wiring and driver complexity. The most realistic path for hybrid ideas at large scale is submodule-level integration, where shading patterns and mismatch can still cause measurable yield losses and hot-spot risk.

Why it matters for cargo bikes and cars. Mobile PV on cargo bikes or cars experiences fast time-varying shadows from trees, buildings, passing objects, and vehicle motion. These conditions create two economic pressures: frequent operation away from the optimum point reduces harvested energy, and repeated thermal stress and potential hot-spots reduce reliability. In this setting, the hybrid approach can be attractive because the crossbar can trigger bypass on a nanosecond to microsecond timescale, protecting cells and stabilizing the string quickly, while the MCU continues a conventional MPPT loop at a slower rate.

Rule-of-thumb guidance. Choose the hybrid approach when shadows are fast and frequent, the PV string current is high enough that bypass conduction losses matter, and you would otherwise need a fast, and more expensive, digital controller to manage active bypass reliably. Choose classical passive bypass when BOM cost and simplicity dominate and shading dynamics are mild; choose classical active bypass when you already require fine-grained digital control and can tolerate the higher sensing and driver complexity.

Table 1. Hardware Cost Comparison (2026 estimates).

System Size	Classical Digital Extra Cost	Hybrid Extra Cost (today)	Hybrid Extra Cost (projected 2028–2030)
Small mobile (200 Wp)	< 3 €	15–30 €	< 5 €
Medium rooftop (5 kWp)	< 15 €	80–150 €	< 25 €
Large utility (100 kWp)	< 300 €	1,500–3,000 €	< 500 €

Table 2. Annual Energy Gain and Payback (realistic urban shading scenario).

Application	Typical Daily Production (classical)	Extra kWh/year (hybrid)	Payback Time (at 0.25 €/kWh)	Additional Benefits
Cargo bike / small car (200 Wp)	0.8–1.2 kWh/day	35–90 kWh/year	4–8 months	+150–450 km range/year, reduced battery cycling
Passenger car roof (400 Wp)	1.6–2.4 kWh/day	70–180 kWh/year	3–7 months	Extended range, lower grid charging cost

Urban rooftop (5 kWp)	4–6 kWh/day	200–500 kWh/year	1.5–3 years	Higher self-consumption, longer module lifetime
Utility-scale (100 kWp)	120–150 MWh/year	6–15 MWh/year	1–2 years	Reduced hot-spot failures, lower O&M cost

Table 3. Annual Energy Gain—a different view.

Application	Typical PV size	Typical PV energy	Shadow dynamics	Hybrid gain (kWh/yr)
Cargo bike canopy / small mobile PV	100–300 Wp	150–400 kWh/yr	Very fast, frequent (trees/buildings)	≈10–60 (≈5–15%)
Car roof PV (auxiliary)	400–800 Wp	500–1,200 kWh/yr	Fast, frequent while driving	≈30–150 (≈5–12%)
Residential rooftop (partially shaded)	3–6 kWp	4,000–9,000 kWh/yr	Mostly slow, occasional fast edges	≈20–250 (≈0.5–3%)
Commercial rooftop (obstructions/HVAC)	50–200 kWp	60,000–300,000 kWh/yr	Mixed; some recurring shade	≈150–2,500 (≈0.2–1%)
Utility-scale PV (well-designed layout)	≥1 MWp	1–2 GWh/yr	Usually mild (unless terrain/poles)	Often small; <0.2% unless shading is significant

Why cars can justify higher cost (value is not only kWh). On vehicles, even modest extra PV energy can have multiple benefits: increased driving range, reduced auxiliary load on the traction battery, less deep cycling, which can improve battery lifetime, and better reliability for onboard electronics. As a rough translation, 50–150 kWh/year of extra PV energy can correspond to about 250–1,000 km/year for an EV consuming about 150–200 Wh/km, or much more for an e-bike or cargo bike using about 10–20 Wh/km.

Note on future opportunity. This section evaluates only the hybrid configuration where the spintronic crossbar manages bypass while a conventional digital controller performs MPPT. A broader opportunity may be to use the crossbar, or a related in-memory compute engine, to assist MPPT itself, especially global-MPP search under partial shading, potentially improving both energy yield and controller simplicity. That case should be treated separately from the present educational hybrid note.

12. Suggested Off-the-Shelf Components for a First Laboratory Demonstrator

This hybrid lecture note assumes a research-grade spintronic crossbar. In early experiments, it is often practical to start with commercially available parts that emulate the same functional blocks, fast per-cell comparison to bypass decision, and then replace the emulator with a real spintronic array when available.

A pragmatic step-by-step lab setup can be built from these off-the-shelf blocks:

- PV source: 4 small cells or 4 clusters on a rig, or a solar simulator / strong lamp to generate repeatable fast shadows.
- DC-DC stage with MPPT-ready control: a development board or evaluation module based on a synchronous boost or buck-boost controller, for example TI LM5176 / LM5122 family or Analog

Devices LT/LTC solar controllers. For a quickest start, a commercial MPPT module can be used as the DC-DC + MPPT block while you prototype the bypass logic.

- String current sensing: a low-ohmic shunt resistor plus current-sense amplifier, for example INA180/INA181 class, feeding the MCU ADC.
- String voltage sensing: resistor divider plus MCU ADC, or an external ADC if higher resolution is needed.
- Per-cell or per-substring voltage sensing: either measure the 5 string nodes N0...N4 with dividers and compute $V_{c1}...V_{c4}$ digitally, or use differential front-ends / instrumentation amplifiers when higher common-mode rejection is required.
- Fast bypass decision emulator before the real crossbar: a resistor network that computes average plus fast comparators, for example LMV331/LM393-class, to produce the four BYPASS_k signals.
- Bypass power stage: low-RDS(on) MOSFETs, often back-to-back for ideal bidirectional bypass, plus appropriate gate driving or level shifting, or isolated gate drivers if the MOSFET is not ground-referenced.
- Low-loss diode replacement option: an ideal diode / smart diode controller or integrated ideal diode device, MOSFET-based, can be used to compare against a Schottky bypass in terms of temperature rise and harvested energy.
- MCU / control platform: a motor-control or power-control MCU, for example TI C2000 class, or an STM32-class MCU is typically sufficient for 100–1,000 Hz MPPT updates; the bypass logic remains asynchronous in the hybrid approach.
- Test/validation tools: an electronic load or battery emulator, oscilloscope with current probe, and a data logger to measure energy over repeated shadow sequences.

Tip for demonstrations: using 4 clusters, each cluster equal to 4 cells in series, raises PV input voltage and makes the DC-DC converter easier to design and more efficient, while still preserving the fast shadow → bypass event → MPPT re-lock behavior discussed in this note.

Acknowledgments: This work was supported by the EIC Pathfinder MultiSpin.AI, grant no. 101130046, by HORIZON-JU-Chips-2025-1-IA NeA1xt grant no. 101194172, and by HORIZON-JU-Chips-2023-1-IA EdgeAI-Trust grant no. 101139892.

Conflicts of Interest: The author is affiliated with Interactive Fully Electrical VehicleS (IFEVS). This technical note is associated with patent applications already filed in Italy. It is presented for educational and scientific discussion at system level.

Table of Acronyms

Acronym	Meaning	Acronym	Meaning
ADC	Analog-to-Digital Converter	MTJ	Magnetic Tunnel Junction
BOM	Bill of Materials	MVM	Matrix-Vector Multiplication
DC-DC	Direct Current to Direct Current	PV	Photovoltaic
MCU	Microcontroller Unit	PWM	Pulse-Width Modulation
MOSFET	Metal-Oxide-Semiconductor Field-Effect Transistor	TIA	Transimpedance Amplifier
MPPT	Maximum Power Point Tracking		

References and Section-by-Section Reference Map

The table below links each report section to a compact set of external references. This is intended as a reading guide for students: each paragraph in a given section is supported by the references listed on the same row, plus any figure captions within that section.

Report section(s)	Main topics	Key references
Abstract, 1	Motivation; fast shadows; why hybrid (crossbar bypass + digital MPPT).	[3,5,9]
2	PV string architecture; boost DC–DC as controllable input impedance; measurement signals.	[1–3]
3	Spintronic crossbar/MTJ basics; analog MVM ($I = G \cdot V$); comparator-style bypass decisions; PROBE recovery concept.	[9–12]
4–5	Why split analog bypass vs digital MPPT; MPPT fundamentals and update-rate limits.	[2–4]
6–7	Interaction between bypass and MPPT; partial shading, local/global maxima; benefits of fast bypass events.	[3,5–7]
8–10	Limitations; alternative architectures; comparison; concluding remarks.	[3,6,9]
11	Economic/energy impact; losses in bypass elements; application-dependent value (mobile PV).	[6–8,12]
12	Off-the-shelf experimentation blocks; emulation strategy; practical lab starting point.	[2,6,12]

References

1. Roger A. Messenger and Jerry Ventre, *Photovoltaic Systems Engineering*, 3rd ed., CRC Press, Boca Raton, FL, 2010.
2. Robert W. Erickson and Dragan Maksimović, *Fundamentals of Power Electronics*, 2nd ed., Springer, Boston, MA, 2001. DOI: 10.1007/978-0-306-48048-5.
3. Trishan Eram and Patrick L. Chapman, "Comparison of Photovoltaic Array Maximum Power Point Tracking Techniques," *IEEE Transactions on Energy Conversion*, vol. 22, no. 2, pp. 439-449, 2007. DOI: 10.1109/TEC.2006.874230.
4. Nicola Femia, Giovanni Petrone, Giovanni Spagnuolo, and Massimo Vitelli, "Optimization of Perturb and Observe Maximum Power Point Tracking Method," *IEEE Transactions on Power Electronics*, vol. 20, no. 4, pp. 963-973, 2005. DOI: 10.1109/TPEL.2005.850975.
5. Hiren Patel and Vivek Agarwal, "Maximum Power Point Tracking Scheme for PV Systems Operating Under Partially Shaded Conditions," *IEEE Transactions on Industrial Electronics*, vol. 55, no. 4, pp. 1689-1698, 2008. DOI: 10.1109/TIE.2008.917118.
6. Romênia G. Vieira, Fábio M. U. de Araújo, Mahmoud Dhimish, and Maria I. S. Guerra, "A Comprehensive Review on Bypass Diode Application on Photovoltaic Modules," *Energies*, vol. 13, no. 10, article 2472, 2020. DOI: 10.3390/en13102472.
7. Boudewijn B. Pannebakker, Arjen C. de Waal, and Wilfried G. J. H. M. van Sark, "Photovoltaics in the Shade: One Bypass Diode per Solar Cell Revisited," *Progress in Photovoltaics: Research and Applications*, vol. 25, no. 10, pp. 836-849, 2017. DOI: 10.1002/pip.2898.
8. J. C. Teo, Rodney H. G. Tan, V. H. Mok, Vigna K. Ramachandaramurthy, and Chia Kwang Tan, "Impact of Bypass Diode Forward Voltage on Maximum Power of a Photovoltaic System under Partial Shading Conditions," *Energy*, vol. 191, article 116491, 2020. DOI: 10.1016/j.energy.2019.116491.

9. Julie Grollier, Damien Querlioz, Kerem Y. Camsari, Karin Everschor-Sitte, Shunsuke Fukami, and Mark D. Stiles, "Neuromorphic Spintronics," *Nature Electronics*, vol. 3, no. 7, pp. 360-370, 2020. DOI: 10.1038/s41928-019-0360-9.
10. Everspin Technologies, "MTJ Storage Element," product technology note, accessed April 2026. No DOI available.
11. William A. Borders, Advait Madhavan, Matthew W. Daniels, Vasileia Georgiou, Martin Lueker-Boden, Tiffany S. Santos, Patrick M. Braganca, Mark D. Stiles, Jabez J. McClelland, and Brian D. Hoskins, "Measurement-driven Neural-Network Training for Integrated Magnetic Tunnel Junction Arrays," *Physical Review Applied*, vol. 21, article 054028, 2024. DOI: 10.1103/PhysRevApplied.21.054028.
12. Salvatore Pennisi, Francesco Pulvirenti, and Amedeo La Scala, "Low-Power Cool Bypass Switch for Hot Spot Prevention in Photovoltaic Panels," *ETRI Journal*, vol. 33, no. 6, pp. 880-886, 2011. DOI: 10.4218/etrij.11.0110.0744.

Disclaimer/Publisher's Note: The statements, opinions and data contained in all publications are solely those of the individual author(s) and contributor(s) and not of MDPI and/or the editor(s). MDPI and/or the editor(s) disclaim responsibility for any injury to people or property resulting from any ideas, methods, instructions or products referred to in the content.